

1 Conflicts are represented in a cognitive space to reconcile domain-general and
2 domain-specific cognitive control

3
4 Guochun Yang,^{1,2,3,4} Haiyan Wu,⁵ Qi Li,⁶ Xun Liu,^{1,2*} Zhongzheng Fu,^{7,8} Jiefeng
5 Jiang^{3,4}

6 ¹ CAS Key Laboratory of Behavioral Science, Institute of Psychology, Beijing
7 100101, China.

8 ² Department of Psychology, University of Chinese Academy of Sciences, Beijing
9 100101, China.

10 ³ Department of Psychological and Brain Sciences, University of Iowa, Iowa City, IA
11 52242, USA.

12 ⁴ Cognitive Control Collaborative, University of Iowa, Iowa City, IA 52242, USA.

13 ⁵ Centre for Cognitive and Brain Sciences and Department of Psychology, University
14 of Macau, Taipa, Macau 999078, China.

15 ⁶ Beijing Key Laboratory of Learning and Cognition, School of Psychology, Capital
16 Normal University, Beijing 100048, China.

17 ⁷ Department of Neurosurgery, Cedars-Sinai Medical Center, Los Angeles, CA
18 90048, USA.

19 ⁸ Division of Humanities and Social Sciences, California Institute of Technology,
20 Pasadena, CA 91125, USA.

21 *Correspondence: liux@psych.ac.cn

22 **Abstract**

23 Cognitive control resolves conflict between task-relevant and -irrelevant information
24 to enable goal-directed behavior. As conflict can arise from different sources (e.g.,
25 sensory input, internal representations), how a finite set of cognitive control processes
26 can effectively address huge array of conflict remains a major challenge. We
27 hypothesize that different conflict can be parameterized and represented as distinct
28 points in a (low-dimensional) cognitive space, which can then be resolved by a
29 limited set of cognitive control processes working along the dimensions. To test this
30 hypothesis, we designed a task with five types of conflict that could be conceptually
31 parameterized along one dimension. Over two experiments, both human performance
32 and fMRI activity patterns in the right dorsolateral prefrontal (dlPFC) support that
33 different types of conflict are organized in a cognitive space. The findings suggest that
34 cognitive space can be a dimension reduction tool to effectively organize neural
35 representations of conflict for cognitive control.

36

37 **Keywords:** cognitive control, cognitive space, domain-general, domain-specific,
38 conflict

39

40 **Introduction**

41 Cognitive control enables humans to behave purposefully by modulating neural
42 processing to resolve conflict between task-relevant and task-irrelevant information.
43 For example, when naming the color of the word “BLUE” printed in red ink, we are
44 likely to be distracted by the word meaning, because reading a word is highly
45 automatic in daily life. To keep our attention on the color, we need to mobilize the
46 cognitive control processes to resolve the conflict between the color and word by
47 boosting/suppressing the processing of color/word meaning. As task-relevant and
48 task-irrelevant information can come from different sources, the sources of conflict
49 and how they should be resolved can vary greatly¹. For example, conflict may occur
50 between items of sensory information, such as between a red light and a police officer
51 signaling cars to pass. Alternatively, conflict may occur between sensory and motor
52 information, such as when a voice on the left asks you to turn right. The large variety
53 of conflict sources implies that there may be unlimited number of conflicts. A key
54 unsolved question in cognitive control is how our brain efficiently resolves a nearly
55 infinite number of different types of conflict.

56 A first step to addressing this question is to examine the commonalities and/or
57 dissociations across different types of conflict that can be categorized into different
58 *domains*. Examples of the domains of conflict include experimental paradigm^{2,3},
59 sensory modality^{4,5}, or conflict type regarding the dimensional overlap of conflict
60 processes^{6,7}.

61 Two solutions to resolving a wide range of conflict types are proposed. They
62 differ based on whether the same cognitive control mechanisms are applied across
63 domains. On the one hand, the *domain-general* cognitive control theories posit that

64 the frontoparietal cortex adaptively encodes task information and can thus flexibly
65 implement control strategies for different types of conflict. This is supported by the
66 generalizable control adjustment (i.e., encountering a conflict trial from one type can
67 facilitate conflict resolution of another type)^{2,8} and similar neural patterns^{9,10} across
68 distinct conflict tasks. A broader domain-general view holds that the frontoparietal
69 brain regions/networks are widely involved in multiple control demands well beyond
70 the conflict domain^{11,12}, which explains the remarkable flexibility in human behaviors.
71 However, since domain-general processes are by definition likely shared by different
72 tasks, when we need to handle multiple task demands at the same time, the efficiency
73 of both tasks would be impaired due to resource competition or interference¹³.
74 Therefore, the domain-general processes is evolutionarily less advantageous for
75 humans to deal with the diverse situations requiring high efficiency¹⁴. On the other
76 hand, the *domain-specific* theories argue that different types of conflict are handled by
77 distinct cognitive control processes (e.g., where and how information processing
78 should be modulated)^{15,16}. However, according to the domain-specific view, the
79 potentially unlimited conflict situations require a large variety of preexisting control
80 processes, which is biologically implausible¹⁷.

81 To reconcile the two theories, researchers recently proposed that cognitive control
82 might be a mixture of domain-general and domain-specific processes. For instance,
83 Freitas et al.¹⁸ found that trial-by-trial adjustment of control can generalize across two
84 conflict domains to different degrees, leading to domain-general (strong
85 generalization) or domain-specific (weak or no generalization) conclusions depending
86 on the task settings of the consecutive conflict. Similarly, different brain networks
87 may show domain-generality (i.e., representing multiple conflicts) or domain-
88 specificity (i.e., representing individual conflicts separately)^{7,19}. Even within the same
89 brain area (e.g., medial frontal cortex), Fu et al.²⁰ found that the neural population
90 activity can be factorized into orthogonal dimensions encoding both domain-general
91 and domain-specific conflict information, which can be selectively read out by
92 downstream brain regions. While the mixture view provides an explanation for the
93 contradictory findings²¹, it suffers the same criticism as domain-specific cognitive
94 control theories, as it still requires unlimited cognitive control processes to fully cover
95 all possible conflicts.

96 A key to reconciling domain-general and domain-specific cognitive control is to
97 organize the nearly infinite possible types of conflict using a system with limited,
98 dissociable dimensions. A construct with a similar function is the *cognitive space*²²,
99 which extends the idea of cognitive map²³ to the representation of abstract
100 information. Critically, the cognitive space view holds that the representations of
101 different abstract information are organized continuously and the locations of
102 representations in the cognitive space are determined by the similarity among the
103 represented information²².

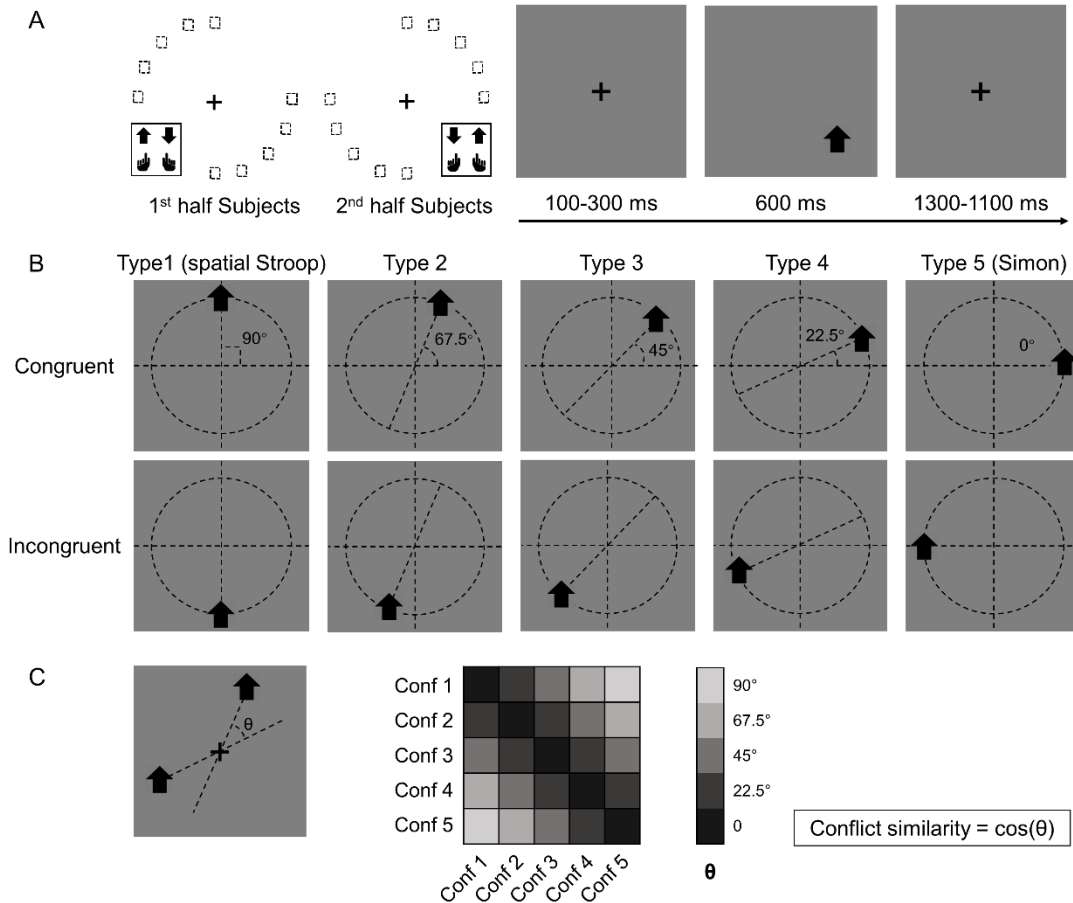
104 In the human brain, it has been shown that abstract^{23,24} and social²⁵ information
105 can be represented in a cognitive space. For example, social hierarchies with two
106 independent scores (e.g., popularity and competence) can be represented in a 2D
107 cognitive space (one dimension for each score), such that each social item can be

108 located by its score in the two dimensions²⁵. In the field of cognitive control, recent
109 studies have begun to conceptualize different control states within a cognitive space²⁶.
110 For example, Fu et al.²⁰ mapped different conflict conditions to locations in a
111 low/high dimensional cognitive space to demonstrate the domain-general/domain-
112 specific problems; Grahek et al.²⁷ used a cognitive space model of cognitive control
113 settings to explain behavioral changes in the speed-accuracy tradeoff. However, the
114 cognitive spaces proposed in these studies were only applicable to a limited number
115 of control states involved in their designs. Therefore, it remains unclear whether there
116 is a cognitive space that can explain an unlimited number of control states, similar to
117 that of the spatial location²² and non-spatial knowledge²³. A challenge to answering
118 this question lies in how to construct control states with continuous levels of
119 similarity. Our recent work²⁸ showed that it is possible to manipulate continuous
120 conflict similarity by using a mixture of two independent conflict types with varying
121 ratios, which can be used to further examine the behavioral and neural evidence for
122 the cognitive space view. It is also unclear how the cognitive space of cognitive
123 control is encoded in the brain, although that of spatial locations and non-spatial
124 abstract knowledge has been relatively well investigated in the medial temporal lobe,
125 medial prefrontal and orbitofrontal system^{22,23}. Recent research has suggested that the
126 abstract task structure could be encoded and implemented by the frontoparietal
127 network^{29,30}, but whether a similar neural system encodes the cognitive space of
128 cognitive control remains untested.

129 We hypothesize that different types of conflict are represented as points in a
130 cognitive space. The dimensions in the cognitive space of conflict can be the
131 aforementioned *domains*, in which domain-specific cognitive control processes are
132 defined. For a specific type of conflict, its location in the cognitive space can be
133 parameterized using a limited number of coordinates, which reflect how much control
134 is needed for each of the domain-specific cognitive control processes. The cognitive
135 space can also represent different types of conflict with low dimensionality^{26,31}.
136 Different domains can be represented conjunctively in a single cognitive space to
137 achieve domain-general cognitive control, as conflict from different sources can be
138 resolved using the same set of cognitive control processes. We further hypothesize
139 that the cognitive space representing different types of conflict may be located in the
140 frontoparietal network due to its essential roles in conflict resolution^{20,32} and abstract
141 task representation³⁰.

142 In this study, we adjusted the paradigm from our previous study²⁸ by including
143 transitions of trials from five different conflict types, which enabled us to test if these
144 conflict types are organized in a cognitive space (Fig. 1A). Specifically, on each trial,
145 an arrow, pointing either upwards or downwards, was presented on one of the 10
146 possible locations on the screen. Participants were required to respond to the pointing
147 direction of the arrow (up or down) by pressing either the left or right key.
148 Importantly, conflict from two sources can occur in this task. On one hand, the
149 vertical location of the arrow can be incongruent with the direction (e.g., an up-
150 pointing arrow on the lower half of the screen), resulting spatial Stroop conflict^{6,33}.
151 On the other hand, the horizontal location of the arrow can be incongruent with the

152 response key (e.g., an arrow requiring left response presented on the right side of the
 153 screen), thus causing Simon conflict^{33,34}. As the arrow location rotates from the
 154 horizontal axis to the vertical axis, spatial Stroop conflict increases, and Simon
 155 conflict decreases. Therefore, the 10 possible locations of the arrow give rise to five
 156 conflict types with unique blend of spatial Stroop and Simon conflict²⁸. As the
 157 increase in spatial Stroop conflict is perfectly correlated with the decrease in Simon
 158 conflict, we can use a 1D cognitive space to represent all five conflict types.



159

160 **Fig. 1. Experimental design.** (A) The left panel shows the orthogonal stimulus-response mappings of
 161 the two participant groups. In each group the stimuli were only displayed at two quadrants of the
 162 circular locations. One group were asked to respond with the left button to the upward arrow and with
 163 the right button to the downward arrow presented in the to-left and bottom-right quadrants, and the
 164 other group vice versa. The right panel shows the time course of one example trial. The stimuli were
 165 displayed for 600 ms, preceded and followed by fixation crosses that lasted for 1400 ms in total. (B)
 166 Examples of the five types of conflict, each containing congruent and incongruent conditions. The
 167 arrows were presented at locations along five orientations with isometric polar angles, in which the
 168 vertical location introduces the spatial Stroop conflict, and the horizontal location introduces the Simon
 169 conflict. Dashed lines are shown only to indicate the location of arrows and were not shown in the
 170 experiments. (C) The definition of the angular difference between two conflict types and the conflict
 171 similarity. The angle θ is determined by the acute angle between two lines that cross the stimuli and the
 172 central fixation. Therefore, stimuli of the same conflict type form the smallest angle of 0, and stimuli

173 between Conflict 1 and Conflict 5 form the largest angle of 90°, and others are in between. Conflict
174 similarity is defined by the cosine value of θ .

175

176 One way to parameterize (i.e., defining a coordinate system) the cognitive space
177 is to encode each conflict type by the angle of the axis connecting its two possible
178 stimulus locations (Fig. 1B). Within this cognitive space, the similarity between two
179 conflict types can be quantified as the cosine value of their angular difference (Fig.
180 1C). If the conflict types are organized as a cognitive space in the brain, the similarity
181 between conflict types in the cognitive space should be reflected in both the behavior
182 and similarity in the neural representations of conflict types. Our data from two
183 experiments using this experimental design support both predictions: using behavioral
184 data, we found that the influence of congruency (i.e., whether the task-relevant and
185 task-irrelevant information indicate the same response) from the previous trial to the
186 next trial increases with the conflict similarity between the two trials. Using fMRI
187 data, we found that more similar conflict showed higher multivariate pattern similarity
188 in the right dorsolateral prefrontal cortex (dlPFC).

189

190 **Results**

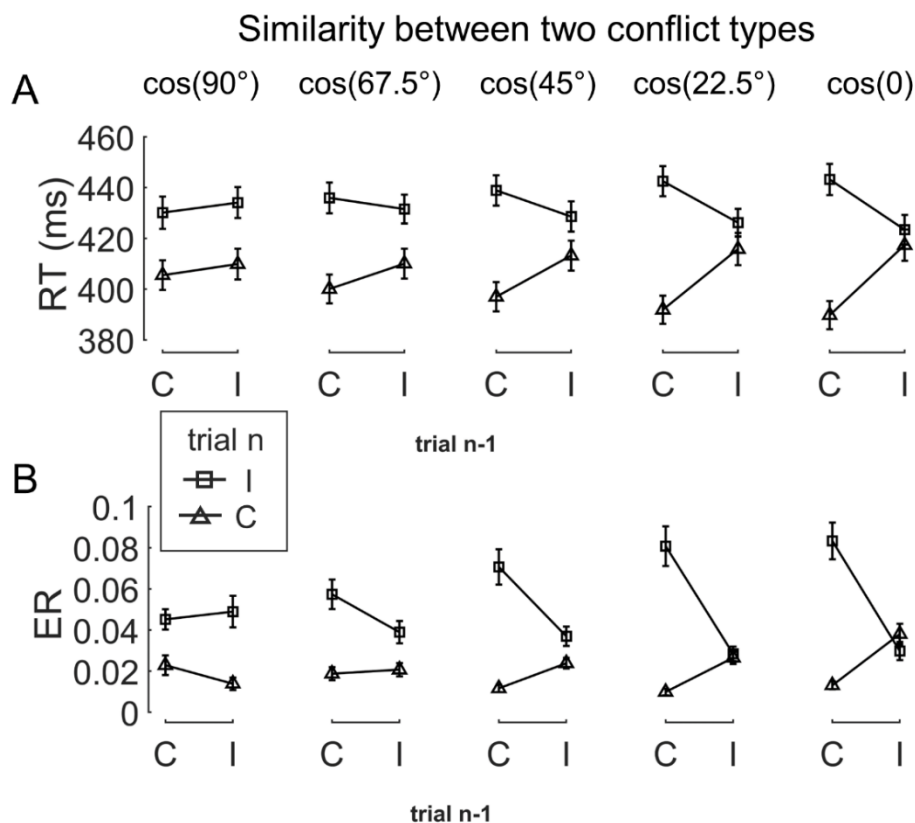
191 *Conflict type similarity modulated behavioral congruency sequence effect (CSE)*

192 Experiment 1.

193 We conducted a behavioral experiment ($n = 33$, 18 females) to examine how CSEs
194 across different conflict types are influenced by their similarity. First, we validated the
195 experimental design by testing the congruency effects. All five conflict types showed
196 robust congruency effects such that the incongruent trials were slower and less
197 accurate than the congruent trials (Note S1; Fig. S1 A/B). To test the influence of
198 similarity between conflict types on behavior, we examined the CSE in consecutive
199 trials. Specifically, the CSE was quantified as the interaction between previous and
200 current trial congruency and can reflect how (in)congruency on the previous trial
201 influences cognitive control on the current trial^{35,36}. It has been shown that the CSE
202 diminishes if the two consecutive trials have different conflict types³⁷⁻³⁹. Similarly, we
203 tested whether the size of CSE increases as a function of conflict similarity between
204 consecutive trials. To this end, we organized trials based on a 5 (previous trial conflict
205 type) \times 5 (current trial conflict type) \times 2 (previous trial congruency) \times 2 (current trial
206 congruency) factorial design, with the first two and the last two factors capturing
207 between-trial conflict similarity and the CSE, respectively. The cells in the 5 \times 5
208 matrix were mapped to different similarity levels according to the angular difference
209 between the two conflict types (Fig. 1C). As shown in Fig. 2, the CSE, measured in
210 both reaction time (RT) and error rate (ER), scaled with conflict similarity.

211 To test the modulation of conflict similarity on the CSE, we constructed a linear
212 mixed effect model to predict RT/ER in each cell of the factorial design using a
213 predictor encoding the interaction between the CSE and conflict similarity (see
214 Methods). The results showed a significant effect of conflict similarity (RT: $\beta = 0.10$

215 ± 0.01 , $t(1978) = 15.82$, $p < .001$, $\eta_p^2 = .120$; ER: $\beta = 0.15 \pm 0.02$, $t(1978) = 7.84$, $p <$
 216 $.001$, $\eta_p^2 = .085$, Fig. S2B/E). In other words, the CSE increased with the conflict
 217 similarity between two consecutive trials. The conflict similarity modulation effect
 218 remained significant after regressing out the influence of physical proximity between
 219 the stimuli of consecutive trials (Note S2). As a control analysis, we also compared
 220 this approach to a two-stage analysis that first calculated the CSE for each previous \times
 221 current trial conflict type condition and then tested the modulation of conflict
 222 similarity on the CSEs²⁸. The two-stage analysis also showed a strong effect of
 223 conflict similarity (RT: $\beta = 0.58 \pm 0.04$, $t(493) = 14.74$, $p < .001$, $\eta_p^2 = .383$; ER: $\beta =$
 224 0.36 ± 0.05 , $t(493) = 7.01$, $p < .001$, $\eta_p^2 = .321$, Fig. S2A/D). Importantly, individual
 225 modulation effects of conflict similarity were positively correlated between the two
 226 approaches (RT: $r = 0.48$; ER: $r = 0.86$, both $ps < 0.003$, one-tailed), indicating the
 227 consistency of the estimated conflict similarity effects across the two approaches.



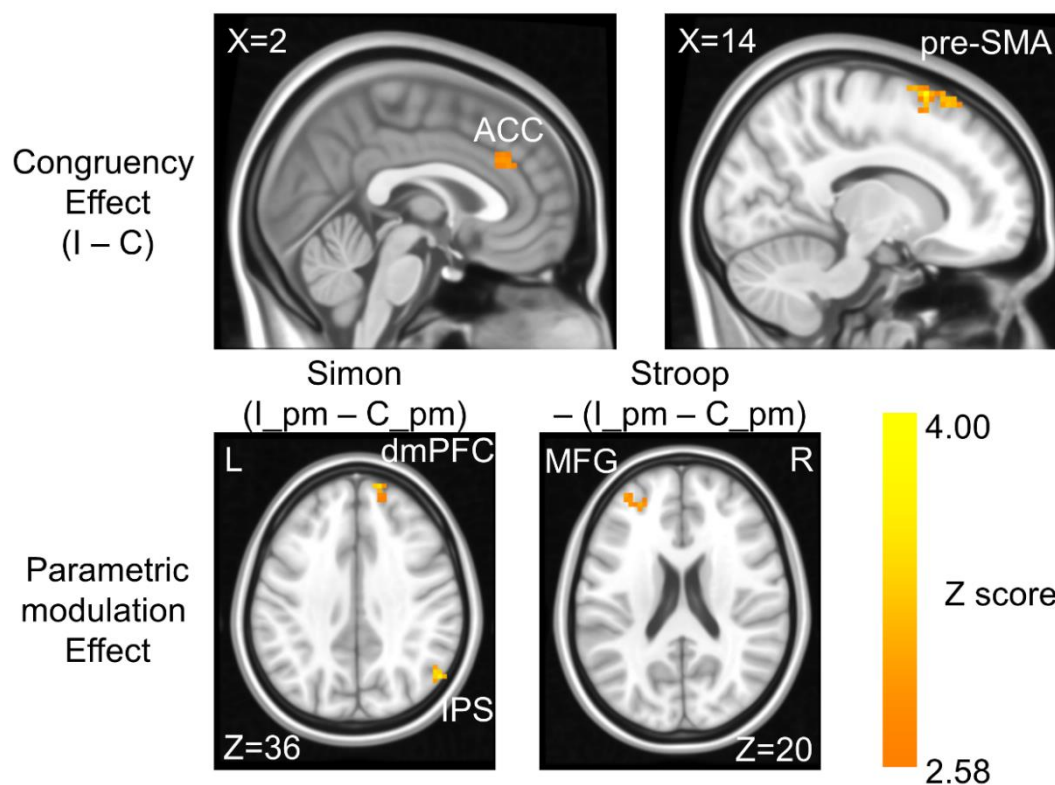
228
 229 **Fig. 2. The conflict similarity modulation on the behavioral CSE in Experiment 1.** (A) RT and (B)
 230 ER are plotted as a function of congruency types on trial n-1 and trial n. Each column shows one
 231 similarity level, as indicated by the defined angular difference between two conflict types. Error bars
 232 are standard errors. C = congruent; I = incongruent; RT = reaction time; ER = error rate.

233
 234 Experiment 2.

235 *Behavioral results.* We next conducted an fMRI experiment using a shorter version of
 236 the same task with a different sample ($n = 35$, 17 females) to seek neural evidence of
 237 how different conflict types are organized. Using behavioral data, we first validated
 238 the experimental design by testing congruency effects in each of the five conflict

239 types (Note S1; Fig. S1 C/D). We then tested the modulation of conflict similarity on
 240 the behavioral CSE using the linear mixed effect model as in Experiment 1 (except
 241 the two-stage method). Results showed a significant effect of conflict similarity
 242 modulation (RT: $\beta = 0.24 \pm 0.04$, $t(1148) = 6.36$, $p < .001$, $\eta_p^2 = .096$; ER: $\beta = 0.33 \pm$
 243 0.06 , $t(1206) = 5.81$, $p < .001$, $\eta_p^2 = .124$, Fig. S2C/F), thus replicating the results of
 244 Experimental 1 and setting the stage for fMRI analysis. As in Experiment 1, the
 245 conflict similarity modulation effect remained significant after regressing out the
 246 influence of physical proximity between the stimuli of consecutive trials (Note S2).

247 *Brain activations modulated by conflict type dissimilarity with univariate analyses*



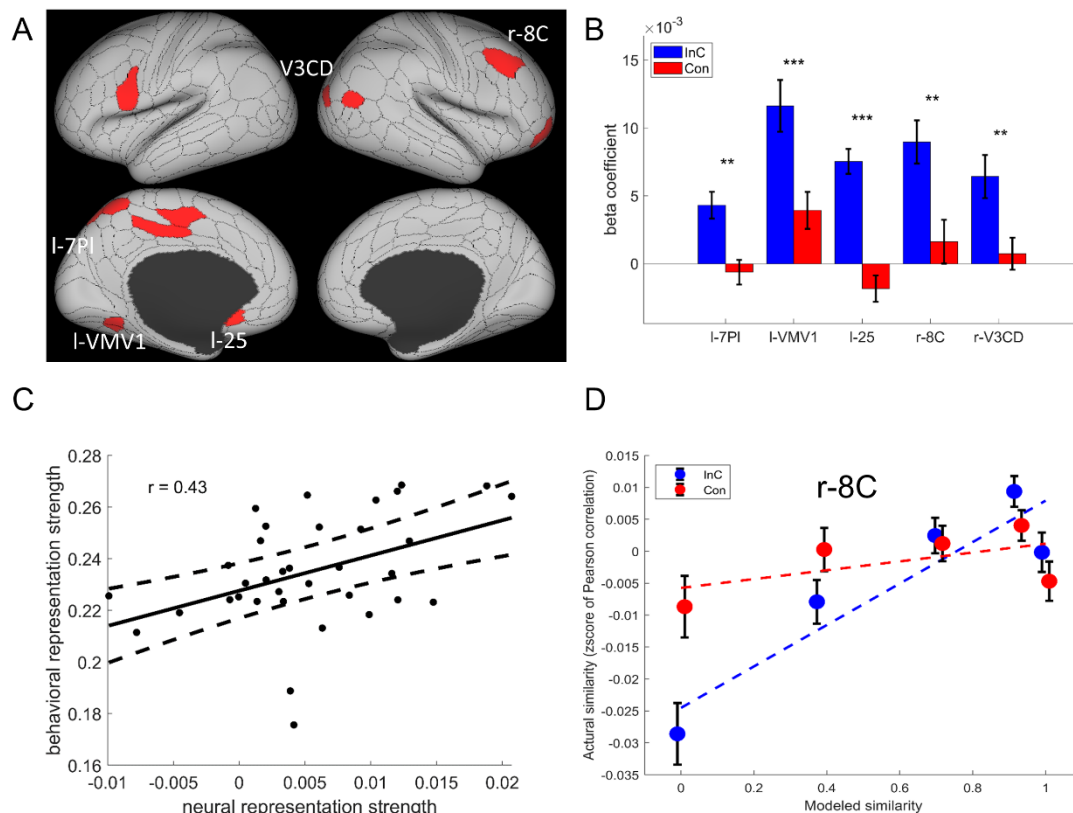
248
 249 **Fig. 3. The congruency effect and parametric modulation effect detected by uni-voxel analyses.**
 250 Results displayed are thresholded with voxel-wise one-tailed $p < .005$ and cluster-size > 20 voxels. The
 251 congruency effect denotes the higher activation in incongruent than congruent condition. The positive
 252 parametric modulation effect ($I_{pm} - C_{pm}$) denotes the higher activation when the conflict type
 253 contained a higher ratio of Simon conflict component (bottom left panel). The negative parametric
 254 modulation effect [converted to positive with $-(I_{pm} - C_{pm})$] denotes the higher activation when the
 255 conflict type contained a higher ratio of spatial Stroop conflict component (bottom right panel). I =
 256 incongruent; C = congruent; pm = parametric modulator.

257
 258 In the fMRI analysis, we first replicated the classic congruency effect by searching for
 259 brain regions showing higher univariate activation in incongruent than congruent
 260 conditions (GLM1, see Methods). Consistent with the literature^{20,40}, this effect was
 261 observed in the pre-supplementary motor area (pre-SMA) and anterior cingulate
 262 cortex (ACC) areas (Fig. 3, Table S1). We then tested the encoding of conflict type as

263 a cognitive space by identifying brain regions with activation levels parametrically
 264 covarying with the coordinates (i.e., axial angle relative to the horizontal axis) in the
 265 hypothesized cognitive space. As shown in Fig. 1B, change in the angle corresponds
 266 to change in spatial Stroop and Simon conflicts in opposite directions. Accordingly, in
 267 the left middle frontal gyrus (MFG), fMRI activation scaled with the increase in
 268 spatial Stroop conflict, whereas the right inferior parietal sulcus (IPS) and the right
 269 dorsomedial prefrontal cortex (dmPFC) displayed positive correlation between fMRI
 270 activation and Simon conflict (Fig. 3, Fig. S3, Table S1).

271 To further test if the univariate results explain the conflict similarity modulation
 272 of the behavioral CSE (slope in Fig. S2C), we conducted brain-behavioral correlation
 273 analyses for regions identified above. Regions with higher spatial Stroop/Simon
 274 modulation effects were expected to trigger higher behavioral conflict similarity
 275 modulation effect on the CSE. However, none of the three regions (i.e., left MFG,
 276 right IPS and right dmPFC, Fig. 3) were positively correlated with the behavioral
 277 performance, all $p_{FDR} > .762$, one-tailed. In addition, since the conflict type difference
 278 covaries with the orientation of the arrow location at the individual level (e.g., the
 279 stimulus in a higher level of Simon conflict is always closer to the horizontal axis, see
 280 Fig. S4), the univariate modulation effects may not reflect purely conflict type
 281 difference. To further tease these factors apart, we used multivariate analyses.

282 *Multivariate patterns of the right dlPFC encodes the conflict similarity*



283
 284 **Fig. 4. The conflict type effect.** (A) Brain regions surviving the FDR-correction ($p_{FDR} < 0.05$ and $p <$
 285 0.001) across the 360 regions (criterion 1). Labeled regions are those meeting the criterion 2. (B) The
 286 regions showing stronger encoding of conflict type in the incongruent than congruent conditions

287 (criterion 2). ** $p_{FDR} < .01$, *** $p_{FDR} < .001$. (C) The brain-behavior correlation of the right 8C
288 (criterion 3). (D) Illustration of the different encoding strength of conflict type similarity in incongruent
289 versus congruent conditions of right 8C. l = left; r = right.

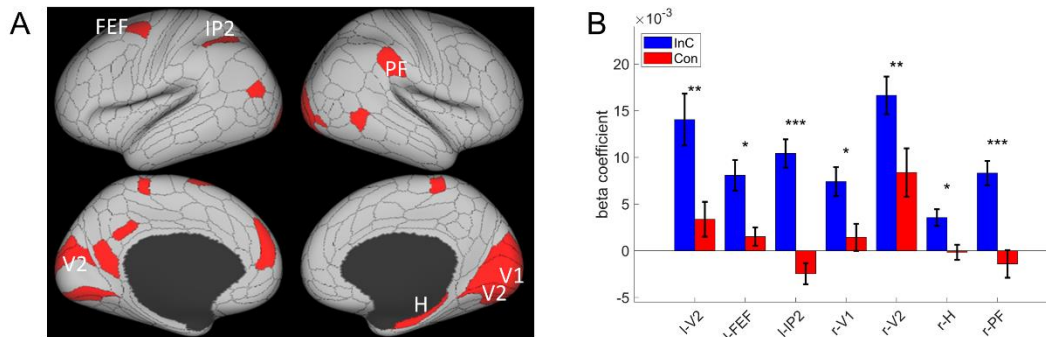
290

291 The hypothesis that the brain encodes conflict types in a cognitive space predicts that
292 similar conflict types will have similar neural representations. To test this prediction,
293 we computed the representational similarity matrix (RSM) that encoded correlations
294 of blood-oxygen-level dependent (BOLD) signal patterns between each pair of
295 conflict type (conflict 1, 2, 3, 4 and 5, as shown in Fig. 1B) \times congruency (congruent,
296 incongruent) \times arrow direction (up, down) \times run \times subject combinations for each of
297 the 360 cortical regions from the Multi-Modal Parcellation (MMP) cortical atlas^{41,42}.
298 The RSM was then submitted to a linear mixed-effect model as the dependent
299 variable to test whether the representational similarity in each region was modulated
300 by various experimental variables (e.g., conflict type, spatial orientation, stimulus,
301 response, etc., see Methods). The linear mixed-effect model was used to de-correlate
302 conflict type and spatial orientation leveraging the between-subject manipulation of
303 stimulus locations (Fig. S4).

304 To validate this method, we applied this analysis to test the effects of
305 response/stimulus features and found that representational similarity of the BOLD
306 signal significantly covaried with whether two response/spatial location/arrow
307 directions were the same most strongly in bilateral motor/visual/somatosensory areas,
308 respectively (Fig. S5). We then identified the cortical regions encoding conflict type
309 as a cognitive space by testing whether their RSMs can be explained by the similarity
310 between conflict types. Specifically, we applied three independent criteria: (1) the
311 cortical regions should exhibit a statistically significant positive conflict similarity
312 effect on the RSM; (2) the conflict similarity effect should be stronger in incongruent
313 than congruent trials to reflect flexible adjustment of cognitive control demand when
314 conflict is present; and (3) the conflict similarity effect should be positively correlated
315 with the behavioral conflict similarity modulation effect on the CSE (see *Behavioral*
316 *Results* of Experiment 2). The first criterion revealed several cortical regions encoding
317 the conflict similarity, including the 8C area (a subregion of dIPFC⁴²), a47r, TPOJ3
318 and V3CD in the right hemisphere, and the 6r, 7Am, 24dd, VMV1, VMV2, 7P1, 23c
319 and 25 areas in the left hemisphere ($p_{FDRS} < 0.05$, with raw $ps < 0.001$, one-tailed, Fig.
320 4A). We next tested whether these regions were related to cognitive control by
321 comparing the strength of conflict similarity effect between incongruent and
322 congruent conditions (criterion 2). Results revealed that the left lateral area 7P (7P1),
323 left ventromedial visual area 1 (VMV1), left dorsal area 24d (24dd), right Brodmann
324 area 8C (8C), and right V3CD met this criterion, $p_{FDRS} < .01$, one-tailed (Table 1, Fig.
325 4B), suggesting that the representation of conflict type was strengthened when
326 conflict was present (e.g., Fig. 4D). The inter-subject brain-behavior correlation
327 analysis (criterion 3) showed that the strength of conflict similarity effect on RSM
328 scaled with the modulation of conflict similarity on the CSE (slope in Fig. S2C) in
329 right 8C ($r = 0.43$, $p_{FDR} = .027$, one-tailed, Fig. 4C) but not in the other regions (all
330 $p_{FDR} > .632$, one-tailed). In addition, we did not find evidence supporting the encoding

331 of congruency in the right 8C area (see Note S5), suggesting that the right 8C area
 332 specifically represents conflict similarity. In sum, we found converging evidence
 333 supporting that the right dlPFC (8C area) encoded conflict similarity, which further
 334 supports the hypothesis that conflict types are represented in a cognitive space.

335 *Multivariate patterns of visual and oculomotor areas encode stimulus orientation*



336 **Fig. 5. The axial orientation effect.** (A) Brain regions surviving the FDR-correction ($p_{FDR} < 0.05$ and
 337 $p < 0.001$) across the 360 regions (criterion 1). Labeled regions are those meeting the criterion 2. (B)
 338 The regions showing stronger encoding of orientation in the incongruent than congruent conditions
 339 (criterion 2). * $p_{FDR} < .05$, ** $p_{FDR} < .01$, *** $p_{FDR} < .001$.

341
 342 To tease apart the representation of conflict type from that of perceptual information,
 343 we tested the modulation of the spatial orientations of stimulus locations on RSM
 344 using the aforementioned RSA. We also applied three independent criteria: (1) the
 345 cortical regions should exhibit a statistically significant orientation effect on the RSM;
 346 (2) the conflict similarity effect should be stronger in incongruent than congruent
 347 trials; and (3) the orientation effect should not interact with the CSE, since the
 348 orientation effect was dissociated from the conflict similarity effect and was not
 349 expected to influence cognitive control. We observed increasing fMRI
 350 representational similarity between trials with more similar orientations of stimulus
 351 location in the occipital cortex, such as right V1, bilateral V2 and V3, right V4, left
 352 area temporoparietooccipital junction 3 (TPOJ3) and right PHT areas (FDR corrected
 353 $ps < 0.05$ and raw $ps < 0.001$). We also found the same effect in several oculomotor
 354 related regions, including the left frontal eye field (FEF), anterior 6m (6ma), area
 355 intraparietal 2 (IP2), right parietal area F (PF) and bilateral 5m, as well as other
 356 regions (Fig. 5A). Then we tested if any of these brain regions were related to the
 357 conflict representation by comparing their encoding strength between incongruent and
 358 congruent conditions. Results showed that the right V1, bilateral V2, left FEF, left
 359 IP2, right hippocampus (H) and right PF encoded stronger orientation effect in the
 360 incongruent than the congruent condition, $p_{FDRs} < .05$, one-tailed (Table1, Fig. 5B).
 361 We then tested if any of these regions was related to the behavioral performance, and
 362 results showed that none of them positively correlated with the behavioral conflict
 363 similarity modulation effect, all $p_{FDR} > .675$, one-tailed. Thus all regions are
 364 consistent with the criterion 3. Like the right 8C area, none of the reported areas
 365 directly encoded congruency (see Note S5). Taken together, we found that the visual

366 and oculomotor regions encoded orientations of stimulus location in a continuous
 367 manner and that the encoding strength was stronger when conflict was present.

368 To explore the relation between conflict type and orientation representations, we
 369 conducted representational connectivity (i.e., the similarity between two RSMs of two
 370 regions)⁴³ analyses and found that among the orientation effect regions, the right V1
 371 and bilateral V2 showed significant representational connectivity with the right 8C
 372 compared to the controlled regions (including those encoding orientation effect but
 373 not showing larger encoding strength in incongruent than congruent conditions, as
 374 well as three other regions encoding none of our defined effects in the main RSA, see
 375 Methods). Compared with the largest connectivity strength in the controlled regions
 376 (i.e., the left V3, $\beta = 0.1447 \pm 0.0069$), we found higher connectivity in the left V2, β
 377 $= 0.1645 \pm 0.0060$, $t(34) = 4.86$, right V1, $\beta = 0.1628 \pm 0.0065$, $t(34) = 4.54$, and
 378 right V2, $\beta = 0.1678 \pm 0.0074$, $t(34) = 5.65$, all $p_{FDR} < .001$, one-tailed (Fig. S6).
 379

380 **Table 1. Summary statistics of regions showing larger encoding strength in**
 381 **incongruent than congruent conditions for the conflict type and**
 382 **orientation effects.**

Region name	$t(34)$	$\beta(SD)$	Cohen's d	p_{FDR}
<i>Conflict type effect</i>				
left 7P1	3.13	0.0049 ± 0.0016	0.53	.011
left VMV1	3.96	0.0077 ± 0.0019	0.67	.002
left 24	7.82	0.0094 ± 0.0012	1.32	< .001
right 8C	3.15	0.0073 ± 0.0023	0.53	.011
right V3CD	2.86	0.0057 ± 0.0020	0.48	.017
<i>Orientation effect</i>				
left V2	3.20	0.0107 ± 0.0033	0.54	.007
left FEF	2.97	0.0066 ± 0.0022	0.50	.010
left IP2	5.73	0.0129 ± 0.0022	0.97	.001
right V1	2.70	0.0060 ± 0.0022	0.46	.014
right V2	3.26	0.0083 ± 0.0025	0.55	.007
right H	2.79	0.0037 ± 0.0013	0.47	.014
right PF	5.31	0.0097 ± 0.0018	0.90	< .001

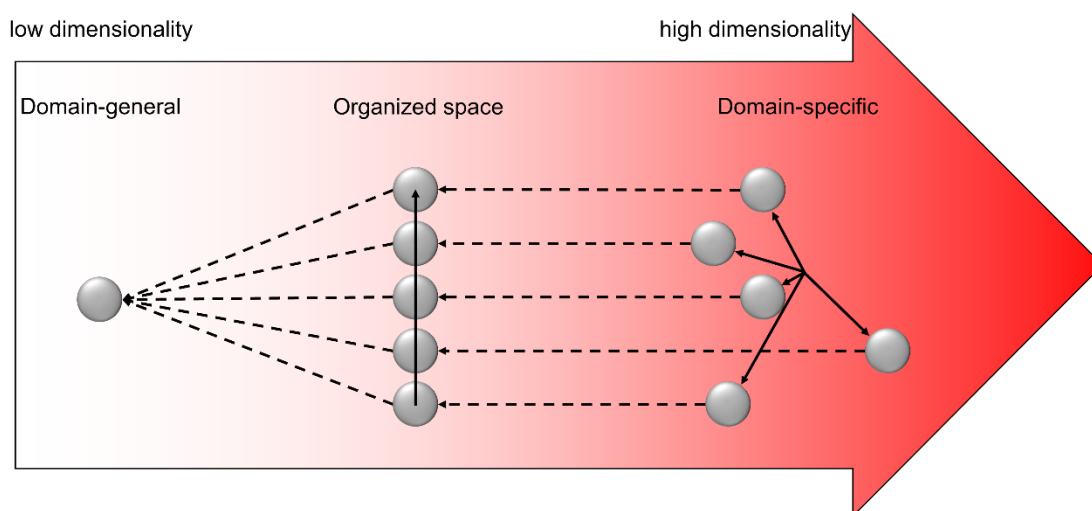
383

384 Discussion

385 Understanding how different types of conflict are resolved is essential to answer how
 386 cognitive control achieves adaptive behavior. However, the dichotomy between
 387 domain-general and/or domain-specific processes presents a dilemma^{15,21}.

388 Reconciliation of the two views also suffers from the inability to fully address how
 389 infinite conflict can be resolved by a limited set of cognitive control processes. In this
 390 study, we hypothesized that this issue can be addressed if conflict is organized as a
 391 cognitive space. Leveraging the well-known dissociation between the spatial Stroop
 392 and Simon conflict⁴⁴⁻⁴⁶, we designed five conflict types that are systematically

393 different from each other. The cognitive space hypothesis predicted that the
 394 representational proximity/distance between two conflict types scales with their
 395 similarities/dissimilarities, which was tested at both behavioral and neural levels.
 396 Behaviorally, we found that the CSEs were linearly modulated by conflict similarity
 397 between consecutive trials, replicating and extending our previous study²⁸. BOLD
 398 activity patterns in the right dlPFC further showed that the representational similarity
 399 between conflict types was modulated by their conflict similarity, and that strength of
 400 the modulation was positively associated with the modulation of conflict similarity on
 401 the behavioral CSE. We also observed that activity in three brain regions (right IPS,
 402 right dlPFC and left MFG) was parametrically modulated by the conflict type
 403 difference, though they did not directly explain the behavioral results. Additionally,
 404 we found that the visual regions encoded the spatial orientation of the stimulus
 405 location, which might provide the essential concrete information to determine the
 406 conflict type. Together, these results support the hypothesis that the conflicts are
 407 organized in a cognitive space that enables a limited set of cognitive control processes
 408 to resolve infinite possible types of conflict.



409
 410 **Fig. 6. Illustration of the hypothesized dimensionalities of different representations.** The shade of
 411 the red color indicates the degree of dimensionality (i.e., how many dimensions are needed to represent
 412 different states). The dimensionality of domain-general representation is extremely low, with all
 413 representations compressed to one dot. The dimensionality of domain-specific representation is
 414 extremely high, with each control state encoded in a unique and orthogonal dimension. The
 415 dimensionality of the organized representation is modest, enabling distant states to be separated but
 416 also allowing close states to share representations. The solid arrows show the axes of different
 417 dimensions. The dashed arrows indicate how the representational dimensionality can be reduced by
 418 projecting the independent dimensions to a common dimension.

419
 420 Conventionally, the domain-general view of control suggests a common
 421 representation for different types of conflict (Fig. 6, left), while the domain-specific
 422 view suggests dissociated representations for different types (Fig. 6, right). Previous
 423 research on this topic often adopts a binary manipulation of conflict²¹ (i.e., each
 424 domain only has one conflict type) and thus is not suitable to test the cognitive space

425 hypothesis. Here, we parametrically manipulated the similarity of conflict in different
426 conflict types and demonstrated that the two theories can be reconciled as a cognitive
427 space²² (Fig. 6, middle). Specifically, the cognitive space provides a solution to use a
428 single cognitive space organization to encode different types of conflict that are close
429 (domain-general) or distant (domain-specific) to each other. It also shows the
430 potential for how unlimited conflict types can be coded using limited resources (i.e.,
431 as different points in a low-dimensional cognitive space). Moreover, geometry can
432 also emerge in the cognitive space²⁰, which will allow for decomposition of a conflict
433 type (e.g., how much conflict in each of the dimensions in the cognitive space) so that
434 it can be mapped into the limited set of cognitive control processes. Such geometry
435 enables fast learning of cognitive control settings from similar conflict types by
436 providing a measure of similarity (e.g., as distance in space).

437 If the dimensionality of the cognitive space of conflict is extremely high, the
438 cognitive space solution would suffer the same criticism as the domain-specificity
439 theory. We argue that the dimensionality is manageable for the human brain, as task
440 information unrelated to differentiating conflicts can be removed. For example, the
441 Simon conflict can be represented in a space consisting of spatial location, stimulus
442 information and responses. Thus, the dimensionality of the cognitive space of conflict
443 should not exceed the number of represented features. The dimensionality can be
444 further reduced, as humans selectively represent a small number of features when
445 learning task representations (e.g., spatial information is reduced to the horizontal
446 dimension from the 3D space we live in)⁴⁷. The reduced dimensionality does not only
447 require less effort to represent the conflict, but also facilitates generalization of
448 cognitive control settings among different conflict types²⁶.

449 Although our finding of cognitive space in the right dlPFC differs from other
450 cognitive space studies^{24,25,48} that highlighted the orbitofrontal and hippocampus
451 regions, it is consistent with the cognitive control literature. The prefrontal cortex has
452 long been believed to be a key region of cognitive control representation⁴⁹⁻⁵¹ and is
453 widely engaged in multiple task demands^{12,52}. However, it is not until recently that the
454 multivariate representation in this region has been examined. For instance, Vaidya et
455 al.²⁹ reported that frontal regions presented latent states that are organized
456 hierarchically. Freund et al.³² showed that dlPFC encoded the target and congruency
457 in a typical color-word Stroop task. Taken together, we suggest that the right dlPFC
458 might flexibly encode a variety of cognitive spaces to meet the dynamic task
459 demands. In addition, we found no such representation in the left dlPFC (Note S6),
460 indicating a possible lateralization. Previous studies showed that the left dlPFC was
461 related to the expectancy-related attentional set up-regulation, while the right dlPFC
462 was related to the online adjustment of control^{53,54}, which is consistent with our
463 findings. Moreover, the right PFC also represents a composition of single rules⁵⁵,
464 which may explain how the spatial Stroop and Simon types can be jointly encoded in
465 a single space.

466 We found that participants with stronger conflict representation as cognitive
467 space in right dlPFC have also adjusted their conflict control to a greater extent based
468 on the conflict similarity (Fig 4C). The finding suggests that the cognitive space

469 organization of conflict guides cognitive control to adjust behavior. Previous studies
470 have shown that participants may adopt different strategies to represent a task, with
471 the model-based strategies benefitting goal-related behaviors more than the model-
472 free strategies⁵⁶. Similarly, we propose that the cognitive space could serve as a
473 mental model to assist fast learning and efficient organization of cognitive control
474 settings. With the organization of a cognitive space, a new conflict can be quickly
475 assigned a location in the cognitive space, which will facilitate the development of
476 cognitive control settings for this conflict by interpolating nearby conflicts and/or
477 projecting the location to axes representing different cognitive control processes. On
478 the other hand, without a cognitive space, there would be no measure of similarity
479 between conflict on different trials, hence limiting the ability of fast learning of
480 cognitive control setting from similar trials.

481 The cognitive space in the right dlPFC appears to be an abstraction of concrete
482 information from the visual regions. We found that the right V1 and bilateral V2
483 encoded the spatial orientation of the target location (Fig. 5) and showed strong
484 representational connectivity with the right dlPFC (Fig. S6), suggesting that there
485 might be information exchange between these regions. We speculate that the
486 representation of spatial orientation may have provided the essential perceptual
487 information to determine the conflict type (Fig. 1) and thus served as the critical input
488 for the cognitive space. The conflict type representation further incorporates the
489 stimulus-response mapping rules to the spatial orientation representation, so that
490 vertically symmetric orientations can be recognized as the same conflict type (Fig.
491 S4). In other words, the representation of conflict type involves the compression of
492 perceptual information⁵⁷, which is consistent with the idea of a low-dimensional
493 representation of cognitive control^{26,31}. The compression and abstraction processes
494 might be why the frontoparietal regions are the top of hierarchy of information
495 processing⁵⁸ and why the frontoparietal regions are widely engaged in multiple task
496 demands⁵⁹.

497 With conventional univariate analyses, we observed that the overall congruency
498 effect was located at the medial frontal regions (i.e., pre-SMA and ACC), which is
499 consistent with previous studies^{20,40}. Beyond that, we also found regions that can be
500 parametrically modulated by conflict type difference, including right IPS, right dlPFC
501 (modulated by Simon difference) and left MFG (modulated by spatial Stroop
502 difference). The lateralization of these regions is consistent with a previous finding¹⁹,
503 which highlighted the difference of Stroop and Simon types with brain activities at
504 different hemispheres. The scaling of brain activities based on conflict difference is
505 potentially important to the representational organization of different types of conflict.
506 However, we didn't observe their brain-behavioral relevance. One possible reason is
507 that the conflict (dis)similarity is a combination of (dis)similarity of spatial Stroop and
508 Simon conflicts, but each univariate region only reflects difference along a single
509 conflict domain. Also likely, the representational geometry is more of a multivariate
510 problem than what univariate activities can capture⁶⁰. Future studies may adopt
511 approaches such as repetition suppression induced fMRI adaptation²⁶ to test the role
512 of univariate activities in task representations.

513 One limitation of this study needs to be noted. To parametrically manipulate the
514 conflict similarity levels, we adopted the spatial Stroop-Simon paradigm that enables
515 parametrical combinations of spatial Stroop and Simon conflicts. However, since this
516 paradigm is a two-alternative forced choice design, the behavioral CSE is not a pure
517 measure of adjusted control but could be partly confounded by bottom-up factors such
518 as feature integration⁶¹. Future studies may replicate our findings with a multiple-
519 choice design with confound-free trial sequences⁶².

520 In sum, we showed that the cognitive control can be organized in an abstract
521 cognitive space that is represented in the right dlPFC and guides cognitive control to
522 adjust goal-directed behavior. The cognitive space hypothesis reconciles the long-
523 standing debate between the domain-general and domain-specific views of cognitive
524 control and provides a parsimonious and more broadly applicable framework for
525 understanding how our brains efficiently and flexibly represents multiple task
526 settings.

527
528

529 **Materials and Methods**

530 *Subjects*

531 In Experiment 1, we enrolled thirty-three college students (19-28 years old, average of
532 21.5 ± 2.3 years old; 19 males). In Experiment 2, thirty-six college students were
533 recruited, and one subject was excluded due to not following task instructions. The
534 final sample of Experiment 2 consisted of thirty-five participants (19-29 years old,
535 average of 22.3 ± 2.5 years old; 17 males). The sample sizes were determined based
536 on our previous study²⁸. All participants reported no history of psychiatric or
537 neurological disorders and were right-handed, with normal or corrected-to-normal
538 vision. The experiments were approved by the Institutional Review Board of the
539 Institute of Psychology, Chinese Academy of Science. Informed consent was obtained
540 from all subjects.

541

542 *Method Details*

543 *Experiment 1*

544 *Experimental Design.* We adopted a modified spatial Stroop-Simon task²⁸ (Fig. 1).
545 The task was programmed with the E-prime 2.0 (Psychological Software Tools, Inc.).
546 The stimulus was an upward or downward black arrow (visual angle of $\sim 1^\circ$)
547 displayed on a 17-inch LCD monitor with a viewing distance of ~ 60 cm. The arrow
548 appeared inside a grey square at one of ten locations with the same distance from the
549 center of the screen, including two horizontal (left and right), two vertical (top and
550 bottom), and six corner (orientations of 22.5° , 45° and 67.5°) locations. The distance
551 from the arrow to the screen center was approximately 3° . To dissociate orientation of

552 stimulus locations and conflict types (see below), participants were randomly
553 assigned to two sets of stimulus locations (one included top-right and bottom-left
554 quadrants, and the other included top-left and bottom-right quadrants).

555 Each trial started with a fixation cross displayed in the center for 100–300 ms,
556 followed by the arrow for 600 ms and another fixation cross for 1100–1300 ms (the
557 total trial length was fixed at 2000 ms). Participants were instructed to respond to the
558 pointing direction of the arrow by pressing a left or right button and to ignore its
559 location. The mapping between the arrow orientations and the response buttons was
560 counterbalanced across participants. The task design introduced two possible sources
561 of conflict: on one hand, the direction of the arrow is either congruent or incongruent
562 with the vertical location of the arrow, thus introducing a spatial Stroop conflict^{33,63},
563 which contains the dimensional overlap between task-relevant stimulus and task-
564 irrelevant stimulus¹; on the other hand, the response (left or right button) is either
565 congruent or incongruent with the horizontal location of the arrow, thus introducing a
566 Simon conflict^{33,34}, which contains the dimensional overlap between task-irrelevant
567 stimulus and response¹. Therefore, the five polar orientations of the stimulus location
568 (from 0 to 90°) defined five unique combinations of spatial Stroop and Simon
569 conflicts, with more similar orientations having more similar composition of conflict.
570 More generally, the spatial orientation of the arrow location relative to the center of
571 the screen forms a cognitive space of different blending of spatial Stroop and Simon
572 conflict.

573 The formal task consisted of 30 runs of 101 trials each, divided into three sessions
574 of ten runs each. The participants completed one session each time and all three
575 sessions within one week. Before each session, the participants performed training
576 blocks of 20 trials repeatedly until the accuracy reached 90% in the most recent block.
577 The trial sequences of the formal task were pseudo-randomly generated to ensure that
578 each of the task conditions and their transitions occurred with equal number of trials.

579 *Experiment 2*

580 *Experimental Design.* The apparatus, stimuli and procedure were identical to
581 Experiment 1 except for the changes below. The stimuli were back projected onto a
582 screen (with viewing angle being ~3.9° between the arrow and the center of the
583 screen) behind the subject and viewed via a surface mirror mounted onto the head
584 coil. Due to the time constraints of fMRI scanning, the trial numbers decreased to a
585 total of 340, divided into two runs with 170 trials each. To obtain a better
586 hemodynamic model fitting, we generated two pseudo-random sequences optimized
587 with a genetic algorithm⁶⁴ conducted by the NeuroDesign package⁶⁵ (see Note S3 for
588 more detail). In addition, we added 6 seconds of fixation before each run to allow the
589 stabilization of the hemodynamic signal, and 20 seconds after each run to allow the
590 signal to drop to the baseline.

591 Before scanning, participants performed two practice sessions. The first one
592 contained 10 trials of center-displayed arrow and the second one contained 32 trials
593 using the same design as the main task. They repeated both sessions until their
594 performance accuracy for each session reached 90%, after which the scanning began.

595 *fMRI Image acquisition and preprocessing*

596 Functional imaging was performed on a 3T GE scanner (Discovery MR750) using
597 echo-planar imaging (EPI) sensitive to BOLD contrast [in-plane resolution of $3.5 \times$
598 3.5 mm^2 , 64×64 matrix, 37 slices with a thickness of 3.5 mm and no interslice skip,
599 repetition time (TR) of 2000 ms, echo-time (TE) of 30 ms, and a flip angle of 90°]. In
600 addition, a sagittal T1-weighted anatomical image was acquired as a structural
601 reference scan, with a total of 256 slices at a thickness of 1.0 mm with no gap and an
602 in-plane resolution of $1.0 \times 1.0 \text{ mm}^2$.

603 Before preprocessing, the first three volumes of the functional images were
604 removed due to the instability of the signal at the beginning of the scan. The
605 anatomical and functional data were preprocessed with the fMRIPrep 20.2.0⁶⁶
606 (RRID:SCR_016216), which is based on Nipype 1.5.1⁶⁷ (RRID:SCR_002502).
607 Specifically, BOLD runs were slice-time corrected using 3dTshift from AFNI
608 20160207⁶⁸ (RRID:SCR_005927). The BOLD time-series were resampled to the
609 MNI152NLin2009cAsym space without smoothing. For a more detailed description
610 of preprocessing, see Note S4. After preprocessing, we resampled the functional data
611 to a spatial resolution of $3 \times 3 \times 3 \text{ mm}^3$. All analyses were conducted in volumetric
612 space, and surface maps are produced with Connectome Workbench
613 (<https://www.humanconnectome.org/software/connectome-workbench>) for display
614 purpose only.

615 *Quantification and Statistical Analysis*

616 *Behavioral analysis*

617 *Experiment 1.* RT and ER were the two dependent variables analyzed. As for RTs,
618 we excluded the first trial of each block (0.9%, for CSE analysis only), error trials
619 (3.8%), trials with RTs beyond three *SDs* or shorter than 200 ms (1.3%) and post-
620 error trials (3.4%). For the ER analysis, the first trial of each block and trials after an
621 error were excluded. To exclude the possible influence of response repetition, we
622 centered the RT and ER data within the response repetition and response alternation
623 conditions separately by replacing condition-specific mean with the global mean for
624 each subject.

625 To examine the modulation of conflict similarity on the CSE, we organized trials
626 based on a 5 (previous trial conflict type) \times 5 (current trial conflict type) \times 2 (previous
627 trial congruency) \times 2 (current trial congruency) factorial design. As conflict similarity
628 is commutative between conflict types, we expected the previous by current trial
629 conflict type factorial design to be a symmetrical (e.g., a conflict 1-conflict 2
630 sequence in theory has the same conflict similarity modulation effect as a conflict 2-
631 conflict 1 sequence), resulting a total of 15 conditions left for the first two factors of
632 the design (i.e., previous \times current trial conflict type). For each previous \times current
633 trial conflict type condition, the conflict similarity between the two trials can be
634 quantified as the cosine of their angular difference. In the current design, there were
635 five possible angular difference levels (0, 22.5° , 42.5° , 67.5° and 90° , see Fig. 1C).

636 We further coded the previous by current trial congruency conditions (hereafter
637 abbreviated as CSE conditions) as CC, CI, IC and II, with the first and second letter
638 encoding the congruency (C) or incongruency (I) on the previous and current trial,
639 respectively. As the CSE is operationalized as the interaction between previous and
640 current trial congruency, it can be rewritten as a contrast of $(CI - CC) - (II - IC)$. In
641 other words, the load of CSE on CI, CC, II and IC conditions is 1, -1, -1 and 1,
642 respectively. To estimate the modulation of conflict similarity on the CSE, we built a
643 regressor by calculating the Kronecker product of the conflict similarity scores of the
644 15 previous \times current trial conflict similarity conditions and the CSE loadings of
645 previous \times current trial congruency conditions. This regressor was regressed against
646 RT and ER data separately, which were normalized across participants and CSE
647 conditions. The regression was performed using a linear mixed-effect model, with the
648 intercept and the slope of the regressor for the modulation of conflict similarity on the
649 CSE as random effects (across both participants and the four CSE conditions). As a
650 control analysis, we built a similar two-stage model²⁸. In the first stage, the CSE [i.e.,
651 $(CI - CC) - (II - IC)$] for each of the previous \times current trial conflict similarity
652 condition was computed. In the second stage, CSE was used as the dependent variable
653 and was predicted using conflict similarity across the 15 previous \times current trial
654 conflict type conditions. The regression was also performed using a linear mixed
655 effect model with the intercept and the slope of the regressor for the modulation of
656 conflict similarity on the CSE as random effects (across participants).

657 *Experiment 2.* Behavioral data was analyzed using the same linear mixed effect model
658 as Experiment 1, with all the CC, CI, IC and II trials as the dependent variable. In
659 addition, to test if fMRI activity patterns may explain the behavioral representations
660 differently in congruent and incongruent conditions, we conducted the same analysis
661 to measure behavioral modulation of conflict similarity on the CSE using congruent
662 (CC and IC) and incongruent (CI and II) trials separately.

663 *Estimation of fMRI activity with univariate general linear model (GLM)*

664 To estimate voxel-wise fMRI activity for each of the experimental conditions, the
665 preprocessed fMRI data of each run were analyzed with the GLM. We conducted
666 three GLMs for different purposes. GLM1 aimed to validate the design of our study
667 by replicating the engagement of frontoparietal activities in conflict processing
668 documented in previous studies^{7,19}, and to explore the cognitive space related regions
669 that were parametrically modulated by the conflict type. Preprocessed functional
670 images were smoothed using a 6-mm FWHM Gaussian kernel. We included
671 incongruent and congruent conditions as main regressors and appended a parametric
672 modulator for each condition. The modulation parameters for Conf 1, Conf 2, Conf 3,
673 Conf 4, and Conf 5 trials were -2, -1, 0, 1 and 2, respectively. In addition, we also
674 added event-related nuisance regressors, including error/missed trials, outlier trials
675 (slower than three SDs of the mean or faster than 200 ms) and trials within two TRs
676 of significant head motion (i.e., outlier TRs, defined as standard DVARS > 1.5 or FD
677 > 0.9 mm from previous TR)⁴¹. On average there were 1.2 outlier TRs for each run.
678 These regressors were convolved with a canonical hemodynamic response function

679 (HRF) in SPM 12 (<http://www.fil.ion.ucl.ac.uk/spm>). We further added volume-level
680 nuisance regressors, including the six head motion parameters, the global signal, the
681 white matter signal, the cerebrospinal fluid signal, and outlier TRs. Low-frequency
682 signal drifts were filtered using a cutoff period of 128 s. The two runs were regarded
683 as different sessions and incorporated into a single GLM to get more power. This
684 yielded two beta maps (i.e., a main effect map and a parametric modulation map) for
685 the incongruent and congruent conditions, respectively and for each subject. At the
686 group level, paired t-tests were conducted between incongruent and congruent
687 conditions, one for the main effect and the other for the parametric modulation effect.
688 Since the spatial Stroop and Simon conflict change in the opposite direction to each
689 other, a positive modulation effect would reflect a higher brain activation when there
690 is more Simon conflict, and a negative modulation effect would reflect a higher brain
691 activation for more spatial Stroop conflict. To avoid confusion, we converted the
692 modulation effect of spatial Stroop to positive by using a contrast of $[-(I_{pm} -$
693 $C_{pm})]$ throughout the results presentation. Results were thresholded by 3dclust
694 function in AFNI⁶⁹ with voxel-wise $p < .005$ and cluster-size > 20 voxels, which was
695 supposed to produce a desirable balance between Type I and II error rates⁷⁰. To
696 visualize the parametric modulation effects, we conducted a similar GLM (GLM2),
697 except we used incongruent and congruent conditions from each conflict type as
698 separate regressors with no parametric modulation. Then we extracted beta
699 coefficients for each regressor and each participant with regions observed in GLM1 as
700 regions of interest, and finally got the incongruent–congruent contrasts for each
701 conflict type at the individual level. We reported the results in Fig. 3, Table S1, and
702 Fig. S3. Visualization of the uni-voxel results was made by the MRICron
703 (<https://www.mccauslandcenter.sc.edu/mricro/mricron/>).

704 The GLM3 aimed to prepare for the representational similarity analysis (see
705 below). There were several differences compared to GLM1. The unsmoothed
706 functional images after preprocessing were used. This model included 20 event-
707 related regressors, one for each of the 5 (conflict type) \times 2 (congruency condition) \times 2
708 (arrow direction) conditions. The event-related nuisance regressors were similar to
709 GLM1, but with additional regressors of response repetition and post-error trials to
710 account for the nuisance inter-trial effects. To fully expand the variance, we
711 conducted one GLM analysis for each run. After this procedure, a voxel-wise fMRI
712 activation map was obtained per condition, run and subject.

713 *Representational similarity analysis (RSA)*

714 To measure the neural representation of conflict similarity, we adopted the RSA.
715 RSAs were conducted on each of the 360 cortical regions of a volumetric version of
716 the MMP cortical atlas⁴². To de-correlate the factors of conflict type and orientation of
717 stimulus location, we leveraged the between-subject manipulation of stimulus
718 locations and conducted RSA in a cross-subject fashion (Fig. S4)^{60,71}. The beta
719 estimates from GLM3 were noise-normalized by dividing the original beta
720 coefficients by the square root of the covariance matrix of the error terms⁷². For each
721 cortical region, we calculated the Pearson's correlations between fMRI activity

722 patterns for each run and each subject, yielding a 1400 (20 conditions \times 2 runs \times 35
723 participants) \times 1400 RSM. The correlations were calculated in a cross-voxel manner
724 using the fMRI activation maps obtained from GLM3 described in the previous
725 section. Similar to the behavioral analyses, we assumed the conflict similarity
726 between two trials is commutative and hence collapsed the RSM along the diagonal and
727 converted the lower triangle into a vector, which was then z-transformed and
728 submitted to a linear mixed effect model as the dependent variable. The linear mixed
729 effect model also included regressors of conflict similarity and orientation similarity.
730 Importantly, conflict similarity was based on how Simon and spatial Stroop conflict
731 are combined and hence was calculated by first rotating all subject's stimulus location
732 to the top-right and bottom-left quadrants, whereas orientation was calculated using
733 original stimulus locations. As a result, the regressors representing conflict similarity
734 and orientation similarity were de-correlated. Similarity between two conditions was
735 measured as the cosine value of the angular difference. Other regressors included a
736 target similarity regressor (i.e., whether the arrow directions were identical), a
737 response similarity regressor (i.e., whether the correct responses were identical); a
738 spatial Stroop distractor regressor (i.e., vertical distance between two stimulus
739 locations); a Simon distractor regressor (i.e., horizontal distance between two stimulus
740 locations). Additionally, we also included three regressors denoting the similarity of
741 Run (i.e., whether two conditions are within the same run), Subject (i.e., whether two
742 conditions are within the same subject), and Group (i.e., whether two conditions are
743 within the same subject group, according to the stimulus-response mapping). We also
744 added two regressors including ROI-mean fMRI activations for each condition of the
745 pair to remove the possible uni-voxel influence on the RSM. A last term was the
746 intercept. The intercept and slopes of the regressors were set as random effects at the
747 subject level. Individual effects for each regressor were also extracted from the model
748 for statistical inference and brain-behavioral correlation analyses. In brain-behavioral
749 analyses, only the RT was used as behavioral measure to be consistent with the fMRI
750 results, where the error trials were regressed out.

751 The statistical significance of these beta estimates was determined with one-
752 sample t-tests (one-tailed). Multiple comparison correction was applied with false
753 discovery rate (FDR) approach⁷³ across all cortical regions ($p_{\text{FDR}} < 0.05$), together
754 with a threshold of 0.001 for each region. To test if the representation strengths are
755 different between congruent and incongruent conditions, we also conducted the RDM
756 analyses using only congruent and incongruent trials separately. Individual effects
757 were extracted from each model and tested using a paired t-test. To visualize the
758 difference, we plotted the effect-related patterns (the predictor multiplied by the slope,
759 plus the residual) as a function of the similarity levels (Fig. 4D).

760 *Representational connectivity analysis*

761 To explore the possible relevance between the conflict type and the orientation
762 effects, we conducted representational connectivity⁴³ between regions showing
763 evidence encoding conflict similarity and orientation similarity. Similar to the RSA
764 mentioned above, the z-transformed RSM vector of each region were extracted and

765 submitted to a mixed linear model, with the RSM of the conflict type region (i.e., the
766 right 8C) as the dependent variable, and the RSM of one of the orientation regions
767 (e.g., bilateral V2) as the predictor. Intercept and the slope of the regressor were set as
768 random effects at the subject level, and individual coefficients of the slope were
769 extracted for further statistical analysis. The mixed effect model was conducted for
770 each pair of regions, respectively. Considering there might be strong intrinsic
771 correlations across the RSMs induced by the nuisance factors, such as the within-
772 subject similarity, we added two sets of regions as control. First, we selected regions
773 without showing any effects of interest (i.e., $q_{FDR} > 0.05$ for all the conflict type,
774 orientation, congruency, target, response, spatial Stroop distractor and Simon
775 distractor effects). Second, we selected regions of orientation effect meeting the first
776 but not the second criterion, to account for the potential correlation between regions
777 of the two partly orthogonal regressors (Fig. S6). Existence of representational
778 connectivity was defined by a higher connectivity slope than any of the control
779 regions with paired-t tests.
780

781 **Acknowledgement**

782 We thank Eliot Hazeltine for valuable comments on a previous version of this
783 manuscript. The work was supported by the National Natural Science Foundation of
784 China and the German Research Foundation (NSFC 62061136001/DFG TRR-169) to
785 X.L. and China Postdoctoral Science Foundation (2019M650884) to G.Y.
786

787 **Reference**

- 788 1. Kornblum, S., Hasbroucq, T., and Osman, A. (1990). Dimensional overlap:
789 cognitive basis for stimulus-response compatibility--a model and taxonomy.
790 *Psychol. Rev.* *97*, 253-270. 10.1037/0033-295x.97.2.253.
- 791 2. Freitas, A.L., Bahar, M., Yang, S., and Banai, R. (2007). Contextual adjustments
792 in cognitive control across tasks. *Psychol. Sci.* *18*, 1040-1043. 10.1111/j.1467-
793 9280.2007.02022.x.
- 794 3. Magen, H., and Cohen, A. (2007). Modularity beyond perception: evidence from
795 single task interference paradigms. *Cogn. Psychol.* *55*, 1-36.
796 10.1016/j.cogpsych.2006.09.003.
- 797 4. Yang, G., Nan, W., Zheng, Y., Wu, H., Li, Q., and Liu, X. (2017). Distinct
798 cognitive control mechanisms as revealed by modality-specific conflict
799 adaptation effects. *J. Exp. Psychol. Hum. Percept. Perform.* *43*, 807-818.
800 10.1037/xhp0000351.
- 801 5. Hazeltine, E., Lightman, E., Schwarb, H., and Schumacher, E.H. (2011). The
802 boundaries of sequential modulations: evidence for set-level control. *J. Exp.*
803 *Psychol. Hum. Percept. Perform.* *37*, 1898-1914. 10.1037/a0024662.
- 804 6. Liu, X., Banich, M.T., Jacobson, B.L., and Tanabe, J.L. (2004). Common and
805 distinct neural substrates of attentional control in an integrated Simon and spatial

- 806 Stroop task as assessed by event-related fMRI. *NeuroImage* 22, 1097-1106.
807 10.1016/j.neuroimage.2004.02.033.
- 808 7. Jiang, J., and Egner, T. (2014). Using neural pattern classifiers to quantify the
809 modularity of conflict-control mechanisms in the human brain. *Cereb Cortex* 24,
810 1793-1805. 10.1093/cercor/bht029.
- 811 8. Kan, I.P., Teubner-Rhodes, S., Drummey, A.B., Nutile, L., Krupa, L., and
812 Novick, J.M. (2013). To adapt or not to adapt: the question of domain-general
813 cognitive control. *Cognition* 129, 637-651. 10.1016/j.cognition.2013.09.001.
- 814 9. Peterson, B.S., Kane, M.J., Alexander, G.M., Lacadie, C., Skudlarski, P., Leung,
815 H.C., May, J., and Gore, J.C. (2002). An event-related functional MRI study
816 comparing interference effects in the Simon and Stroop tasks. *Brain Res. Cogn.*
817 *Brain Res.* 13, 427-440. 10.1016/s0926-6410(02)00054-x.
- 818 10. Wu, T., Spagna, A., Chen, C., Schulz, K.P., Hof, P.R., and Fan, J. (2020).
819 Supramodal Mechanisms of the Cognitive Control Network in Uncertainty
820 Processing. *Cereb. Cortex* 30, 6336-6349. 10.1093/cercor/bhaa189 %J Cerebral
821 Cortex.
- 822 11. Assem, M., Glasser, M.F., Van Essen, D.C., and Duncan, J. (2020). A Domain-
823 General Cognitive Core Defined in Multimodally Parcellated Human Cortex.
824 *Cereb. Cortex* 30, 4361-4380. 10.1093/cercor/bhaa023.
- 825 12. Cole, M.W., Reynolds, J.R., Power, J.D., Repovs, G., Anticevic, A., and Braver,
826 T.S. (2013). Multi-task connectivity reveals flexible hubs for adaptive task
827 control. *Nat. Neurosci.* 16, 1348-1355. 10.1038/nn.3470.
- 828 13. Musslick, S., and Cohen, J.D. (2021). Rationalizing constraints on the capacity
829 for cognitive control. *Trends Cogn Sci* 25, 757-775. 10.1016/j.tics.2021.06.001.
- 830 14. Cosmides, L., and Tooby, J. (1994). Origins of domain specificity: The evolution
831 of functional organization. In *Mapping the mind: Domain specificity in cognition*
832 *and culture*, L.A. Hirschfeld, and S.A. Gelman, eds. (Cambridge University
833 Press).
- 834 15. Egner, T. (2008). Multiple conflict-driven control mechanisms in the human
835 brain. *Trends Cogn. Sci.* 12, 374-380. 10.1016/j.tics.2008.07.001.
- 836 16. Kim, C., Chung, C., and Kim, J. (2012). Conflict adjustment through domain-
837 specific multiple cognitive control mechanisms. *Brain Res.* 1444, 55-64.
838 10.1016/j.brainres.2012.01.023.
- 839 17. Abrahamse, E., Braem, S., Notebaert, W., and Verguts, T. (2016). Grounding
840 cognitive control in associative learning. *Psychol. Bull.* 142, 693-728.
841 10.1037/bul0000047.
- 842 18. Freitas, A.L., and Clark, S.L. (2015). Generality and specificity in cognitive
843 control: conflict adaptation within and across selective-attention tasks but not
844 across selective-attention and Simon tasks. *Psychol. Res.* 79, 143-162.
845 10.1007/s00426-014-0540-1.
- 846 19. Li, Q., Yang, G., Li, Z., Qi, Y., Cole, M.W., and Liu, X. (2017). Conflict
847 detection and resolution rely on a combination of common and distinct cognitive
848 control networks. *Neurosci. Biobehav. Rev.* 83, 123-131.
849 10.1016/j.neubiorev.2017.09.032.

- 850 20. Fu, Z., Beam, D., Chung, J.M., Reed, C.M., Mamelak, A.N., Adolphs, R., and
851 Rutishauser, U. (2022). The geometry of domain-general performance monitoring
852 in the human medial frontal cortex. *Science* 376, eabm9922.
853 10.1126/science.abm9922.
- 854 21. Braem, S., Abrahamse, E.L., Duthoo, W., and Notebaert, W. (2014). What
855 determines the specificity of conflict adaptation? A review, critical analysis, and
856 proposed synthesis. *Front. Psychol.* 5, 1134. 10.3389/fpsyg.2014.01134.
- 857 22. Bellmund, J.L.S., Gardenfors, P., Moser, E.I., and Doeller, C.F. (2018).
858 Navigating cognition: Spatial codes for human thinking. *Science* 362.
859 10.1126/science.aat6766.
- 860 23. Behrens, T.E.J., Muller, T.H., Whittington, J.C.R., Mark, S., Baram, A.B.,
861 Stachenfeld, K.L., and Kurth-Nelson, Z. (2018). What Is a Cognitive Map?
862 Organizing Knowledge for Flexible Behavior. *Neuron* 100, 490-509.
863 10.1016/j.neuron.2018.10.002.
- 864 24. Schuck, N.W., Cai, M.B., Wilson, R.C., and Niv, Y. (2016). Human Orbitofrontal
865 Cortex Represents a Cognitive Map of State Space. *Neuron* 91, 1402-1412.
866 10.1016/j.neuron.2016.08.019.
- 867 25. Park, S.A., Miller, D.S., Nili, H., Ranganath, C., and Boorman, E.D. (2020). Map
868 Making: Constructing, Combining, and Inferring on Abstract Cognitive Maps.
869 *Neuron* 107, 1226-1238 e1228. 10.1016/j.neuron.2020.06.030.
- 870 26. Badre, D., Bhandari, A., Keglovits, H., and Kikumoto, A. (2021). The
871 dimensionality of neural representations for control. *Curr Opin Behav Sci* 38, 20-
872 28. 10.1016/j.cobeha.2020.07.002.
- 873 27. Grahek, I., Leng, X., Fahey, M.P., Yee, D., and Shenhav, A. (2022). Empirical
874 and Computational Evidence for Reconfiguration Costs During Within-Task
875 Adjustments in Cognitive Control. In 44.
- 876 28. Yang, G., Xu, H., Li, Z., Nan, W., Wu, H., Li, Q., and Liu, X. (2021). The
877 congruency sequence effect is modulated by the similarity of conflicts. *J. Exp.*
878 *Psychol. Learn. Mem. Cogn.* 47, 1705-1719. 10.1037/xlm0001054.
- 879 29. Vaidya, A.R., Jones, H.M., Castillo, J., and Badre, D. (2021). Neural
880 representation of abstract task structure during generalization. *Elife* 10, 1-26.
881 10.7554/eLife.63226.
- 882 30. Vaidya, A.R., and Badre, D. (2022). Abstract task representations for inference
883 and control. *Trends Cogn Sci* 26, 484-498. 10.1016/j.tics.2022.03.009.
- 884 31. MacDowell, C.J., Tafazoli, S., and Buschman, T.J. (2022). A Goldilocks theory
885 of cognitive control: Balancing precision and efficiency with low-dimensional
886 control states. *Curr Opin Neurobiol* 76, 102606. 10.1016/j.conb.2022.102606.
- 887 32. Freund, M.C., Bugg, J.M., and Braver, T.S. (2021). A Representational Similarity
888 Analysis of Cognitive Control during Color-Word Stroop. *J. Neurosci.* 41, 7388-
889 7402. 10.1523/JNEUROSCI.2956-20.2021.
- 890 33. Lu, C.H., and Proctor, R.W. (1995). The influence of irrelevant location
891 information on performance: A review of the Simon and spatial Stroop effects.
892 *Psychon Bull Rev* 2, 174-207. 10.3758/BF03210959.

- 893 34. Simon, J.R., and Small, A.M., Jr. (1969). Processing auditory information:
894 interference from an irrelevant cue. *J. Appl. Psychol.* 53, 433-435.
895 10.1037/h0028034.
- 896 35. Egner, T. (2007). Congruency sequence effects and cognitive control. *Cogn.*
897 *Affect. Behav. Neurosci.* 7, 380-390. 10.3758/cabn.7.4.380.
- 898 36. Schmidt, J.R., and Weissman, D.H. (2014). Congruency sequence effects without
899 feature integration or contingency learning confounds. *PLoS One* 9, e102337.
900 10.1371/journal.pone.0102337.
- 901 37. Torres-Quesada, M., Funes, M.J., and Lupianez, J. (2013). Dissociating
902 proportion congruent and conflict adaptation effects in a Simon-Stroop
903 procedure. *Acta Psychol. (Amst.)* 142, 203-210. 10.1016/j.actpsy.2012.11.015.
- 904 38. Akcay, C., and Hazeltine, E. (2011). Domain-specific conflict adaptation without
905 feature repetitions. *Psychon Bull Rev* 18, 505-511. 10.3758/s13423-011-0084-y.
- 906 39. Egner, T., Delano, M., and Hirsch, J. (2007). Separate conflict-specific cognitive
907 control mechanisms in the human brain. *NeuroImage* 35, 940-948.
908 10.1016/j.neuroimage.2006.11.061.
- 909 40. Botvinick, M.M., Cohen, J.D., and Carter, C.S. (2004). Conflict monitoring and
910 anterior cingulate cortex: an update. *Trends Cogn. Sci.* 8, 539-546.
911 10.1016/j.tics.2004.10.003.
- 912 41. Jiang, J., Wang, S.F., Guo, W., Fernandez, C., and Wagner, A.D. (2020).
913 Prefrontal reinstatement of contextual task demand is predicted by separable
914 hippocampal patterns. *Nat Commun* 11, 2053. 10.1038/s41467-020-15928-z.
- 915 42. Glasser, M.F., Coalson, T.S., Robinson, E.C., Hacker, C.D., Harwell, J., Yacoub,
916 E., Ugurbil, K., Andersson, J., Beckmann, C.F., Jenkinson, M., et al. (2016). A
917 multi-modal parcellation of human cerebral cortex. *Nature* 536, 171-178.
918 10.1038/nature18933.
- 919 43. Kriegeskorte, N., Mur, M., and Bandettini, P. (2008). Representational similarity
920 analysis - connecting the branches of systems neuroscience. *Front Syst Neurosci*
921 2, 4. 10.3389/neuro.06.004.2008.
- 922 44. Li, Q., Nan, W., Wang, K., and Liu, X. (2014). Independent processing of
923 stimulus-stimulus and stimulus-response conflicts. *PLoS One* 9, e89249.
924 10.1371/journal.pone.0089249.
- 925 45. Wang, K., Li, Q., Zheng, Y., Wang, H., and Liu, X. (2014). Temporal and
926 spectral profiles of stimulus-stimulus and stimulus-response conflict processing.
927 *NeuroImage* 89, 280-288. 10.1016/j.neuroimage.2013.11.045.
- 928 46. Liu, X., Park, Y., Gu, X., and Fan, J. (2010). Dimensional overlap accounts for
929 independence and integration of stimulus-response compatibility effects. *Atten.*
930 *Percept. Psychophys.* 72, 1710-1720. 10.3758/APP.72.6.1710.
- 931 47. Niv, Y. (2019). Learning task-state representations. *Nat Neurosci* 22, 1544-1553.
932 10.1038/s41593-019-0470-8.
- 933 48. Constantinescu, A.O., O'Reilly, J.X., and Behrens, T.E.J. (2016). Organizing
934 conceptual knowledge in humans with a gridlike code. *Science* 352, 1464-1468.
935 10.1126/science.aaf0941.

- 936 49. Miller, E.K., and Cohen, J.D. (2001). An integrative theory of prefrontal cortex
937 function. *Annu. Rev. Neurosci.* 24, 167-202. 10.1146/annurev.neuro.24.1.167.
- 938 50. Milner, B. (1963). Effects of Different Brain Lesions on Card Sorting - Role of
939 Frontal Lobes. *Arch Neurol-Chicago* 9, 90-&. DOI
940 10.1001/archneur.1963.00460070100010.
- 941 51. Mansouri, F.A., Buckley, M.J., and Tanaka, K. (2007). Mnemonic function of the
942 dorsolateral prefrontal cortex in conflict-induced behavioral adjustment. *Science*
943 318, 987-990. 10.1126/science.1146384.
- 944 52. Duncan, J. (2010). The multiple-demand (MD) system of the primate brain:
945 mental programs for intelligent behaviour. *Trends Cogn. Sci.* 14, 172-179.
946 10.1016/j.tics.2010.01.004.
- 947 53. Vanderhasselt, M.A., De Raedt, R., and Baeken, C. (2009). Dorsolateral
948 prefrontal cortex and Stroop performance: tackling the lateralization. *Psychon*
949 *Bull Rev* 16, 609-612. 10.3758/PBR.16.3.609.
- 950 54. Friehs, M.A., Klaus, J., Singh, T., Frings, C., and Hartwigsen, G. (2020).
951 Perturbation of the right prefrontal cortex disrupts interference control.
952 *NeuroImage* 222, 117279. 10.1016/j.neuroimage.2020.117279.
- 953 55. Reverberi, C., Gorgen, K., and Haynes, J.D. (2012). Compositionality of rule
954 representations in human prefrontal cortex. *Cereb Cortex* 22, 1237-1246.
955 10.1093/cercor/bhr200.
- 956 56. Rmus, M., Ritz, H., Hunter, L.E., Bornstein, A.M., and Shenhav, A. (2022).
957 Humans can navigate complex graph structures acquired during latent learning.
958 *Cognition* 225, 105103. 10.1016/j.cognition.2022.105103.
- 959 57. Flesch, T., Juechems, K., Dumbalska, T., Saxe, A., and Summerfield, C. (2022).
960 Orthogonal representations for robust context-dependent task performance in
961 brains and neural networks. *Neuron*. 10.1016/j.neuron.2022.01.005.
- 962 58. Gilbert, C.D., and Li, W. (2013). Top-down influences on visual processing. *Nat*
963 *Rev Neurosci* 14, 350-363. 10.1038/nrn3476.
- 964 59. Duncan, J. (2013). The structure of cognition: attentional episodes in mind and
965 brain. *Neuron* 80, 35-50. 10.1016/j.neuron.2013.09.015.
- 966 60. Freund, M.C., Etzel, J.A., and Braver, T.S. (2021). Neural Coding of Cognitive
967 Control: The Representational Similarity Analysis Approach. *Trends Cogn. Sci.*
968 25, 622-638. 10.1016/j.tics.2021.03.011.
- 969 61. Hommel, B., Proctor, R.W., and Vu, K.P. (2004). A feature-integration account
970 of sequential effects in the Simon task. *Psychol. Res.* 68, 1-17. 10.1007/s00426-
971 003-0132-y.
- 972 62. Braem, S., Bugg, J.M., Schmidt, J.R., Crump, M.J.C., Weissman, D.H.,
973 Notebaert, W., and Egner, T. (2019). Measuring Adaptive Control in Conflict
974 Tasks. *Trends Cogn. Sci.* 23, 769-783. 10.1016/j.tics.2019.07.002.
- 975 63. MacLeod, C.M. (1991). Half a century of research on the Stroop effect: an
976 integrative review. *Psychol. Bull.* 109, 163-203.
- 977 64. Wager, T.D., and Nichols, T.E. (2003). Optimization of experimental design in
978 fMRI: a general framework using a genetic algorithm. *NeuroImage* 18, 293-309.
979 10.1016/S1053-8119(02)00046-0.

- 980 65. Durnez, J., Blair, R., and Poldrack, R.A. (2018). Neurodesign: Optimal
981 Experimental Designs for Task fMRI. *BioRxiv*, 119594. 10.1101/119594.
- 982 66. Esteban, O., Markiewicz, C.J., Blair, R.W., Moodie, C.A., Isik, A.I., Erramuzpe,
983 A., Kent, J.D., Goncalves, M., DuPre, E., Snyder, M., et al. (2019). fMRIPrep: a
984 robust preprocessing pipeline for functional MRI. *Nat. Methods* *16*, 111-116.
985 10.1038/s41592-018-0235-4.
- 986 67. Gorgolewski, K., Burns, C.D., Madison, C., Clark, D., Halchenko, Y.O.,
987 Waskom, M.L., and Ghosh, S.S. (2011). Nipype: a flexible, lightweight and
988 extensible neuroimaging data processing framework in python. *Front.*
989 *Neuroinform.* *5*, 13. 10.3389/fninf.2011.00013.
- 990 68. Jenkinson, M., Bannister, P., Brady, M., and Smith, S. (2002). Improved
991 Optimization for the Robust and Accurate Linear Registration and Motion
992 Correction of Brain Images. *NeuroImage* *17*, 825-841. 10.1006/nimg.2002.1132.
- 993 69. Cox, R.W., and Hyde, J.S. (1997). Software tools for analysis and visualization of
994 fMRI data. *NMR Biomed.* *10*, 171-178. 10.1002/(sici)1099-
995 1492(199706/08)10:4/5<171::Aid-nbm453>3.0.Co;2-I.
- 996 70. Lieberman, M.D., and Cunningham, W.A. (2009). Type I and Type II error
997 concerns in fMRI research: re-balancing the scale. *Soc. Cogn. Affect. Neurosci.*
998 *4*, 423-428. 10.1093/scan/nsp052.
- 999 71. van Baar, J.M., Chang, L.J., and Sanfey, A.G. (2019). The computational and
1000 neural substrates of moral strategies in social decision-making. *Nat. Commun.* *10*,
1001 1483. 10.1038/s41467-019-09161-6.
- 1002 72. Nili, H., Wingfield, C., Walther, A., Su, L., Marslen-Wilson, W., and
1003 Kriegeskorte, N. (2014). A toolbox for representational similarity analysis. *PLoS*
1004 *Comput. Biol.* *10*, e1003553. 10.1371/journal.pcbi.1003553.
- 1005 73. Genovese, C.R., Lazar, N.A., and Nichols, T. (2002). Thresholding of statistical
1006 maps in functional neuroimaging using the false discovery rate. *NeuroImage* *15*,
1007 870-878. 10.1006/nimg.2001.1037.